

Vanishing effective mass of the neutrinoless double beta decay including light sterile neutrinos

Y.F. Li ^{a 1} and Si-shuo Liu ^{b 2}

^a Institute of High Energy Physics, Chinese Academy of Sciences, Beijing 100049, China

^b Department of Modern Physics, University of Science and Technology of China, Hefei, Anhui 230026, China

Abstract

Light sterile neutrinos with masses at the sub-eV or eV scale are hinted by current experimental and cosmological data. Assuming the Majorana nature of these hypothetical particles, we discuss their effects in the neutrinoless double beta decay by exploring the implications of a vanishing effective Majorana neutrino mass $\langle m \rangle_{ee}$. Allowed ranges of neutrino masses, mixing angles and Majorana CP-violating phases are illustrated in some instructive cases for both normal and inverted mass hierarchies of three active neutrinos.

PACS number(s): 14.60.Pq, 25.30.Pt, 14.60.St

¹E-mail: liyufeng@ihep.ac.cn

²E-mail: thingdx@mail.ustc.edu.cn

1 Introduction

Despite the success of the standard three-neutrino oscillations in explaining the results of solar, atmospheric, reactor and accelerator neutrino experiments [1] by two distinct mass-squared differences, a number of anomalies from the short base-line antineutrino experiments (e.g., LSND [2] and MiniBooNE [3]) and the latest reactor antineutrino fluxes [4] indicate the existence of oscillations with much shorter baselines. This would imply the existence of extra mass-squared differences and therefore the mixing of active neutrinos with extra sterile neutrino states [5, 6]. Furthermore, the analysis [7] of cosmic microwave background and large scale structure data is hinting an existence of additional radiation in the Universe, with sterile neutrinos being one of the plausible candidates. Finally, one extra sterile neutrino is also allowed and even favored from a recent analysis of the Big Bang Nucleosynthesis bound [8]. Therefore, we should be open-minded on their existence and it might be instructive to study the light sterile neutrino hypothesis with other oscillation channels [9] or in non-oscillation processes including the beta decay [10] and neutrinoless double beta decay [11, 12].

The most promising process to probe the Majorana nature of massive neutrinos and acquire the information of Majorana CP-violating phases is the neutrinoless double beta decay ($0\nu\beta\beta$) [12, 13] of some even-even nuclei:

$$A(Z, N) \rightarrow A(Z + 2, N - 2) + 2e^-, \quad (1)$$

which takes place via the exchange of Majorana neutrinos but would be prohibited if neutrinos are the Dirac particles. The decay rate is proportional to an effective Majorana neutrino mass term $\langle m \rangle_{ee}$ and to the associated nuclear matrix element. The latter can in principle be calculated with some uncertainties [15] in nuclear physics. The effective neutrino mass $\langle m \rangle_{ee}$ is related to the neutrino masses, mixing angles and Majorana CP phases as follows:

$$\langle m \rangle_{ee} = \left| \sum_i m_i V_{ei}^2 \right|, \quad (2)$$

where m_i is the mass of the i^{th} neutrino mass state and the sum of i includes all light neutrino mass states. V_{ei} stands for an element in the first row of the lepton flavor mixing matrix, and it contains a Majorana CP phase in general.

Great efforts have been made to search for signals of the $0\nu\beta\beta$ process [12, 13] recently, however, only negative results have been obtained and the upper bound on the effective neutrino mass is achieved accordingly (i.e., $\langle m \rangle_{ee} \lesssim 0.3 - 1.0$ eV [14]). Although a positive $0\nu\beta\beta$ signal would verify the Majorana nature of massive neutrinos, negative results do not necessarily mean that neutrinos are the Dirac particles. For Majorana neutrinos, a vanishing effective neutrino mass $\langle m \rangle_{ee}$ due to cancelation among different mass eigenstates could also lead to the failure of $0\nu\beta\beta$ observations. This possibility in the standard scenario of three-neutrino mixing has been explored in some previous works [16, 17]. If light (sub-eV) sterile neutrinos exist and are mixed with their active counterparts, they will also contribute to the $0\nu\beta\beta$ decay rate and modify the prediction on the effective neutrino mass $\langle m \rangle_{ee}$. Therefore, the parameter space of a vanishing $\langle m \rangle_{ee}$ will get altered drastically in contrast to the standard scenario. This point constitutes the main concern of the present work. We shall derive the correlative relations among neutrino masses,

mixing angles and Majorana CP phases and constrain the corresponding parameters by using current experimental data of active and sterile neutrino oscillations.

The main part of this work is organized as follows. In section 2, we shall describe the theoretical framework and derive the analytical formulas for a vanishing $\langle m \rangle_{ee}$. Section 3 is devoted to a numerical analysis. The analytical relations will be confronted with current global oscillation data and numerical examples will be illustrated in several specific cases. Finally, we conclude in section 4.

2 Analytical Calculations

Assuming that neutrinos are the Majorana particles and there exist N_s species of light sterile neutrinos, the neutrino flavor eigenstates $(\nu_e, \nu_\mu, \nu_\tau)$ are connected with the $3 + N_s$ mass eigenstates $(\nu_i, i = 1, \dots, 3 + N_s)$ by a $3 \times (3 + N_s)$ flavor mixing matrix V in the charged-current interactions, which contains $3 + 3N_s$ mixing angles, $1 + 2N_s$ Dirac CP phases and $2 + N_s$ Majorana CP phases. In the $0\nu\beta\beta$ process, as revealed in Eq. (2), only the mixing matrix elements in the first row of V are relevant in our calculations. Without loss of generality, we may redefine the phases of three charged lepton fields in an appropriate way such that the phase of the mixing matrix element V_{ei} is only of the Majorana type. So the expression for the effective neutrino mass $\langle m \rangle_{ee}$ can be rewritten as

$$\langle m \rangle_{ee} = \left| m_1 |V_{e1}|^2 e^{2i\rho_1} + m_2 |V_{e2}|^2 e^{2i\rho_2} + m_3 |V_{e3}|^2 + \sum_{j=4}^{3+N_s} m_j |V_{ej}|^2 e^{2i\rho_j} \right|, \quad (3)$$

where ρ_i ($i = 1, \dots, 3 + N_s$) are the Majorana phases and a vanishing ρ_3 has been chosen. Although some schemes with more than one sterile neutrino may have their distinct properties such as CP violating effects in active-sterile neutrino oscillations [5, 6], we can combine all the sterile neutrino contributions in the $0\nu\beta\beta$ process by assuming an effective $(3 + 1)$ scheme in which the additional neutrino mass m_0 , mixing matrix element $|V_{e0}|$ and Majorana CP phase ρ_0 are defined by

$$m_0 |V_{e0}|^2 e^{2i\rho_0} \equiv \sum_{j=4}^{3+N_s} m_j |V_{ej}|^2 e^{2i\rho_j}. \quad (4)$$

Taking account of Eq. (3) and (4), we find that a vanishing effective neutrino mass (i.e., $\langle m \rangle_{ee} = 0$) requires

$$\begin{aligned} m_0 |V_{e0}|^2 \sin 2\rho_0 + m_1 |V_{e1}|^2 \sin 2\rho_1 + m_2 |V_{e2}|^2 \sin 2\rho_2 &= 0, \\ m_0 |V_{e0}|^2 \cos 2\rho_0 + m_1 |V_{e1}|^2 \cos 2\rho_1 + m_2 |V_{e2}|^2 \cos 2\rho_2 + m_3 |V_{e3}|^2 &= 0. \end{aligned} \quad (5)$$

Comparing these two conditions with current experimental data on the mixing matrix elements ($|V_{e1}|$, $|V_{e2}|$, $|V_{e3}|$ and $|V_{e0}|$) and the mass-squared differences ($\Delta m_{21}^2 \equiv m_2^2 - m_1^2$, $\Delta m_{31}^2 \equiv m_3^2 - m_1^2$ and $\Delta m_{01}^2 \equiv m_0^2 - m_1^2$), we might be allowed to determine or constrain the absolute neutrino mass scale, neutrino mass hierarchies and Majorana CP phases. Before doing the most general analysis, however, let us discuss several specific cases to reveal the main consequences of Eq. (5).

(a) The case of $m_0 = 0$ or $|V_{e0}| = 0$ (or both) means that contributions to $\langle m \rangle_{ee}$ are canceled out among different sterile species of the mass eigenstates, which is practically equivalent to the standard scenario of three-neutrino mixing. Taking the $(3 + 2)$ scheme with two additional sterile neutrinos as an example, the cancelation between ν_4 and ν_5 indicates

$$\frac{m_4}{m_5} = -\frac{|V_{e5}|^2}{|V_{e4}|^2}, \quad |\rho_5 - \rho_4| = \frac{2n+1}{2}\pi, \quad (6)$$

with n being an arbitrary non-negative integer. In this case, a vanishing $\langle m \rangle_{ee}$ only requires the parameter correlations among three active neutrinos,

$$\frac{m_1}{m_2} = -\frac{|V_{e2}|^2 \sin 2\rho_2}{|V_{e1}|^2 \sin 2\rho_1}, \quad \frac{m_2}{m_3} = +\frac{|V_{e3}|^2 \sin 2\rho_1}{|V_{e2}|^2 \sin (2\rho_2 - 2\rho_1)}, \quad (7)$$

which have already been studied in some earlier literatures [16, 17]. Therefore, we shall only discuss the $0\nu\beta\beta$ process with non-vanishing sterile neutrino contributions in the following parts of this work.

(b) The case of CP invariance requires that all the Majorana CP phases should take some specific values (i.e., $\rho_i = n_i\pi/2$ with n_i being arbitrary integers). So the two conditions in Eq. (5) will be simplified to a single one,

$$(-1)^{l_0}m_0|V_{e0}|^2 + (-1)^{l_1}m_1|V_{e1}|^2 + (-1)^{l_2}m_2|V_{e2}|^2 + m_3|V_{e3}|^2 = 0, \quad (8)$$

with $l_k = 0$ or 1 for $(k = 0, 1, 2)$, depending on n_k being even or odd integers respectively. Thus the mass spectrum of active and sterile neutrinos might be fully determined for each group of (l_0, l_1, l_2) with the help of current knowledge on neutrino mass-squared differences and mixing matrix elements. A simple calculation shows that $(0, 1, 0)$ and $(1, 0, 1)$ are permitted for both mass hierarchies of active neutrinos, $(1, 0, 0)$ and $(0, 1, 1)$ are allowed only for the case of $\Delta m_{31}^2 > 0$, but all the other possibilities are ruled out by current global neutrino data.

(c) The case of a neutrino mass eigenstate being massless depends on the sign of Δm_{31}^2 . $m_1 = 0$ or $m_3 = 0$ might hold for normal or inverted mass hierarchies respectively. If $\Delta m_{31}^2 > 0$ and $m_1 = 0$ hold, then Eq. (5) requires

$$\frac{m_2}{m_0} = -\frac{|V_{e0}|^2 \sin 2\rho_0}{|V_{e2}|^2 \sin 2\rho_2}, \quad \frac{m_3}{m_0} = +\frac{|V_{e0}|^2 \sin (2\rho_0 - 2\rho_2)}{|V_{e3}|^2 \sin 2\rho_2}; \quad (9)$$

on the other hand, in the case of $\Delta m_{31}^2 < 0$ and $m_3 = 0$, we are led to

$$\frac{m_2}{m_0} = -\frac{|V_{e0}|^2 \sin (2\rho_0 - 2\rho_1)}{|V_{e2}|^2 \sin (2\rho_2 - 2\rho_1)}, \quad \frac{m_1}{m_0} = +\frac{|V_{e0}|^2 \sin (2\rho_0 - 2\rho_2)}{|V_{e1}|^2 \sin (2\rho_2 - 2\rho_1)}. \quad (10)$$

Since the masses of active neutrinos are totally calculable when we assume $m_1 = 0$ or $m_3 = 0$, part of the parameter space of Majorana CP phases must be excluded. Furthermore, the allowed region of $(m_0, |V_{e0}|)$ might be constrained either by using Eq. (9) or Eq. (10) from the active neutrino data or by using Eq. (4) from the sterile neutrino data. Therefore, a comparison between the two sectors may test the conditions of $\langle m \rangle_{ee} = 0$ and give complete constraints on the $(m_0, |V_{e0}|)$ parameter space.

In addition to the special cases considered above, we can derive the most general results about $(m_0, |V_{e0}|)$ and ρ_0 from the conditions in Eq. (5). Indeed,

$$m_0^2 |V_{e0}|^4 = m_1^2 |V_{e1}|^4 + m_2^2 |V_{e2}|^4 + m_3^2 |V_{e3}|^4 + 2m_1 m_2 |V_{e1}|^2 |V_{e2}|^2 \cos(2\rho_1 - 2\rho_2) \\ + 2m_1 m_3 |V_{e1}|^2 |V_{e3}|^2 \cos 2\rho_1 + 2m_2 m_3 |V_{e2}|^2 |V_{e3}|^2 \cos 2\rho_2, \quad (11)$$

as well as

$$\tan 2\rho_0 = \frac{m_1 |V_{e1}|^2 \sin 2\rho_1 + m_2 |V_{e2}|^2 \sin 2\rho_2}{m_1 |V_{e1}|^2 \cos 2\rho_1 + m_2 |V_{e2}|^2 \cos 2\rho_2 + m_3 |V_{e3}|^2}. \quad (12)$$

Note from Eq. (11) and Eq. (12) that the parameters of sterile neutrinos (i.e., $m_0 |V_{e0}|^2$ and ρ_0) may be calculated from the active neutrino data, depending on the absolute neutrino mass scale and neutrino mass hierarchies. On the other hand, we may directly constrain $m_0 |V_{e0}|^2$ and ρ_0 from the sterile neutrino data by using Eq. (4). A combined analysis of both sectors will give the complete parameter space allowed by the global neutrino data.

3 Numerical Analysis

To be explicit, let us carry out a numerical analysis of the implications of $\langle m \rangle_{ee} = 0$. For illustration, we shall take the $(3 + 2)$ neutrino mixing scheme with two sub-eV sterile neutrinos as an example, which is more or less favored by the latest experimental [5, 6] and cosmological data [7]. We may also assume that these sterile neutrinos under consideration do not significantly affect the values of two mass-squared differences and three mixing angles of active neutrinos extracted from current active neutrino data [18, 19]. In this assumption we shall use the latest results on active neutrino parameters in Ref. [18] and sterile neutrino data in Ref. [5], namely, $\Delta m_{21}^2 \approx 7.58 \times 10^{-5} \text{ eV}^2$, $\Delta m_{31}^2 \approx 2.39 (-2.31) \times 10^{-3} \text{ eV}^2$, $\Delta m_{41}^2 \approx 0.47 \text{ eV}^2$ and $\Delta m_{51}^2 \approx 0.87 \text{ eV}^2$ together with $|V_{e1}| \approx 0.824$, $|V_{e2}| \approx 0.547$, $|V_{e3}| \approx 0.145$, $|V_{e4}| \approx 0.128$ and $|V_{e5}| \approx 0.138$ ¹ as typical inputs of the best-fit values. The sign of Δm_{31}^2 is unknown and the absolute neutrino mass scale, which can be characterized by the smallest neutrino mass (m_1 for $\Delta m_{31}^2 > 0$ or m_3 for $\Delta m_{31}^2 < 0$), is expected to be at most of $\mathcal{O}(0.1) \text{ eV}$ or $\mathcal{O}(1) \text{ eV}$ as constrained by current experimental and cosmological data [1, 20]. On the other hand, the Majorana CP phases are totally unconstrained and will vary in the full parameter space. Finally, we shall take into account the uncertainties of active neutrino parameters at the 1σ or 3σ confident level in our numerical analysis but neglect the uncertainties of sterile neutrino parameters which are not explicitly presented in Ref. [5]. We admit that our calculations are quite preliminary and mainly serve for illustration, but it should be emphasized that they indeed reveal the main consequences of $\langle m \rangle_{ee} = 0$.

Now we are able to do the numerical analysis on possible implications of $\langle m \rangle_{ee} = 0$. We shall employ the analytical results of different cases discussed in section 2 as our guidelines and plot the corresponding regions allowed by the global oscillation data.

In the cases of the smallest neutrino mass being zero, it is straightforward to present the correlative relations among different Majorana CP phases and between $(m_0, |V_{e0}|)$. First we illustrate the case of $m_1 = 0$ in Fig. 1. The parameter space of two Majorana

¹An analysis of the latest global data has also been done by a few independent groups, such as Ref. [19] for the standard three-neutrino oscillations and Ref. [6] for the active-sterile neutrino oscillations.

phases (ρ_0, ρ_2) is shown in Fig. 1(a), where different (black and grey) colors stand for 1σ and 3σ ranges of the active neutrino parameters respectively. One should note that ρ_1 is irrelevant in this case because the massless mass eigenstate ν_1 does not contribute to the $0\nu\beta\beta$ process. In Fig 1(a), we can learn that there are two isolated regions to guarantee $\langle m \rangle_{ee} = 0$, and they are related through the transformation of $(\rho_0 \rightarrow \pi - \rho_0, \rho_2 \rightarrow \pi - \rho_2)$. This point can be understood by considering the fact that the formulas in Eq. (9) are invariant under the same transformation. Furthermore, the allowed regions can be generalized to the larger $(\rho_0 + n_0\pi, \rho_2 + n_2\pi)$ parameter space, where n_0 and n_2 are arbitrary integers. The allowed regions of $(m_0, |V_{e0}|)$ can be found in Fig. 1(b), where the (black and grey) shaded regions stand for constraints from the active neutrino data and the region with (red) sparse lines is required by the sterile neutrino parameters. The (black) horizontal line stands for the 2σ upper bound on the sum of the neutrino masses from cosmological probes [21] and only the region below this line is allowed. The profiles of these allowed regions have the shape of the inverse-rate curve in the single logarithmic scale, which can be easily understood by the analytical expressions in Eq. (4) and Eq. (5). One should also note that there is no overlap between the allowed regions of active and sterile neutrino data even within the 3σ ranges, indicating that the case of $m_1 = 0$ and $\Delta m_{31}^2 > 0$ is disfavored by current global oscillation data if $\langle m \rangle_{ee} = 0$ holds. This conclusion demonstrates the fact that the minimum of $m_0|V_{e0}|^2$ from the sterile neutrino data, $|\sqrt{\Delta m_{41}^2}|V_{e4}|^2 - \sqrt{\Delta m_{51}^2}|V_{e5}|^2|$ is always larger than the maximum of $m_0|V_{e0}|^2$ from the active neutrino data, $|\sqrt{\Delta m_{21}^2}|V_{e2}|^2 + \sqrt{\Delta m_{31}^2}|V_{e3}|^2|$.

A similar analysis for $\Delta m_{31}^2 < 0$ and $m_3 = 0$ is given in Fig. 2. The allowed regions of Majorana CP phases and $(m_0, |V_{e0}|)$ are illustrated in the upper and lower panels respectively. Only the differences of Majorana phases can be constrained because it is the third mass eigenstate ν_3 that decouples from the effective mass $\langle m \rangle_{ee}$ due to its masslessness. In Fig. 2(a), we take $(\rho_0 - \rho_1)$ and $(\rho_2 - \rho_1)$ as free parameters and find that they are strongly correlated and constrained. The area of the allowed region here is much smaller than that in Fig. 1(a) simply for the reason that the mixing matrix elements of active neutrinos in Eq. (10) (i.e., $|V_{e1}|, |V_{e2}|$) are much more precise than that appearing only in Eq. (9) (i.e., $|V_{e3}|$). Now let us take a look at Fig. 2(b) for the allowed regions of $(m_0, |V_{e0}|)$. The (black) horizontal line stands for the 2σ upper bound on the sum of the neutrino masses from cosmological probes [21]. Its most distinct difference from Fig. 1(b) is the overlaps between active and sterile neutrino constraints appearing at both 1σ and 3σ levels. Therefore, $m_3 = 0$ and $\langle m \rangle_{ee} = 0$ can be simultaneously satisfied in the presence of sub-eV sterile neutrinos. In the meantime, it is instructive to compare the present scenario with the standard scenario of three-neutrino mixing, where a vanishing $\langle m \rangle_{ee}$ favors $\Delta m_{31}^2 > 0$ over $\Delta m_{31}^2 < 0$.

So far we have only discussed the consequences of a vanishing $\langle m \rangle_{ee}$ in some specific cases. To illustrate the dependence on the absolute neutrino mass scale, we calculate the allowed ranges of $m_0|V_{e0}|^2$ versus the smallest neutrino mass (m_1 or m_3) for both neutrino mass hierarchies in Fig. 3. We give the constraints from the active neutrino data with (black and grey) shaded regions and constraints from the sterile neutrino data with regions of (red) sparse lines. The overlapping regions of both sectors are the complete parameter space of $\langle m \rangle_{ee} = 0$ and the global oscillation data. The case of $\Delta m_{31}^2 > 0$ is illustrated in Fig. 3(a), which confirms the previous conclusion that the specific case of $m_1 = 0$ is disfavored by current global oscillation data. As m_1 is getting larger, the active neutrino spectrum changes from the hierarchical type to the quasi-degenerate one

and therefore the relations between $m_0|V_{e0}|^2$ and m_1 in Eq. (11) approximate to linear functions. Numerically, we may find the allowed ranges explicitly as $0.005 \text{ eV} \lesssim m_1 \lesssim 0.116 \text{ eV}$ and $0.006 \text{ eV} \lesssim m_0|V_{e0}|^2 \lesssim 0.029 \text{ eV}$. In comparison, a similar calculation for $\Delta m_{31}^2 < 0$ can be found in Fig. 3(b) and the ranges of m_3 and $m_0|V_{e0}|^2$ are $0 \lesssim m_3 \lesssim 0.10 \text{ eV}$ and $0.012 \text{ eV} \lesssim m_0|V_{e0}|^2 \lesssim 0.029 \text{ eV}$, respectively. Finally, let us comment on the Majorana CP phase ρ_0 in Eq. (12). Although it can be calculated from the active neutrino data, there is no correlation between ρ_0 and the absolute mass scale (characterized by m_1 or m_3). Our numerical calculation shows that ρ_0 may run over the full parameter space at each point of the smallest neutrino mass (m_1 or m_3). Only when the neutrino mass scale is fixed, as the specific cases discussed above, there can be non-trivial correlations among different Majorana CP phases. Within the full parameter ranges, it is instructive to estimate the minimal value of the effective Majorana mass (i.e., $\langle m \rangle_{ee}^{\min}$) where $\langle m \rangle_{ee}$ does not vanish. We calculate $\langle m \rangle_{ee}^{\min}$ versus the smallest neutrino mass (m_1 or m_3) for both $\Delta m_{31}^2 > 0$ and $\Delta m_{31}^2 < 0$ cases in Fig. 4. The black solid and grey dashed lines stand for 1σ and 3σ ranges of the active neutrino data respectively. When $\Delta m_{31}^2 > 0$ holds, there are two separated ranges of m_1 for a non-vanishing $\langle m \rangle_{ee}^{\min}$. A hierarchical neutrino mass spectrum with $m_1 \lesssim 10^{-3} \text{ eV}$ predicts a minimal value of $\langle m \rangle_{ee}$ as $(3 \sim 4) \times 10^{-3} \text{ eV}$ and the magnitude of $\langle m \rangle_{ee}^{\min}$ can reach the $\mathcal{O}(0.1) \text{ eV}$ level for a nearly degenerate spectrum of the active neutrinos. In contrast, a non-vanishing $\langle m \rangle_{ee}^{\min}$ can only be achieved for $m_3 \gtrsim 0.1 \text{ eV}$ in the case of $\Delta m_{31}^2 < 0$ and $\langle m \rangle_{ee}^{\min}$ grows as m_3 becomes larger.

4 Concluding Remarks

Motivated by non-observation of the $0\nu\beta\beta$ process and possible hints of sub-eV sterile neutrinos from the latest experimental and cosmological data, we have discussed the implications of a vanishing effective Majorana mass (i.e., $\langle m \rangle_{ee} = 0$) in the presence of light sterile neutrinos. Current neutrino oscillation data from both active and sterile neutrinos do allow $\langle m \rangle_{ee} = 0$ to hold if neutrinos are the Majorana particles and their masses, mixing angles and Majorana CP phases possess some specific correlations. The allowed parameter space can be drastically altered in contrast to that of the standard three-neutrino mixing scenario. For the standard scenario, a vanishing $\langle m \rangle_{ee}$ favors $\Delta m_{31}^2 > 0$ over $\Delta m_{31}^2 < 0$. However, it is not really the case after we include the light sterile neutrino contributions. In the specific case where the smallest neutrino mass vanishes, a vanishing $\langle m \rangle_{ee}$ is consistent with the case of $\Delta m_{31}^2 < 0$ rather than $\Delta m_{31}^2 > 0$. Furthermore, for the complete parameter ranges, both cases are allowed and we may constrain the smallest neutrino mass as $0.005 \text{ eV} \lesssim m_1 \lesssim 0.116 \text{ eV}$ and $0 \lesssim m_3 \lesssim 0.10 \text{ eV}$ respectively.

Going beyond the Standard Model, there are different mechanisms [22] that may be able to mediate the $0\nu\beta\beta$ process, including light (active and sterile) Majorana neutrinos, heavy sterile Majorana neutrinos [23, 24] and other particles [25] that can induce the lepton-number-violating (LNV) interactions. We stress that we have simply neglected all the contributions other than light Majorana neutrinos and our conclusions will be invalid once other mechanisms can give a comparable decay rate as either light active neutrinos or light sterile neutrinos. In addition, when more accurate data on neutrino mass and mixing parameters and more sensitive observations or constraints on the $0\nu\beta\beta$ process are achieved in the future [26, 27], it might be possible to confirm or rule out the parameter space we have obtained and even probe the existence of light sterile neutrino states.

We would like to thank Prof. Zhi-zhong Xing for suggesting this topic and very helpful discussions. One of us (SXL) is also indebted to him for the warm hospitality and financial support at the theoretical physics division, Institute of High Energy Physics in Beijing, where this work was done. YFL is supported by the China Postdoctoral Science Foundation under grant No. 20100480025.

References

- [1] Particle Data Group, K. Nakamura *et al.*, J. Phys. G **37**, 075021 (2010).
- [2] A. Aguilar *et al.* (LSND Collaboration), Phys. Rev. D **64**, 112007 (2001).
- [3] A.A. Aguilar-Arevalo *et al.* (MiniBooNE Collaboration), Phys. Rev. Lett. **105**, 181801 (2010).
- [4] G. Mention *et al.*, Phys. Rev. D **83**, 073006 (2011); P. Huber, Phys. Rev. C **84**, 024617 (2011).
- [5] J. Kopp, M. Maltoni and T. Schwetz, Phys. Rev. Lett. **107**, 091801 (2011).
- [6] C. Giunti and M. Laveder, arXiv:1107.1452 [hep-ph]; arXiv:1109.4033 [hep-ph].
- [7] J. Hamann *et al.*, Phys. Rev. Lett. **105**, 181301 (2010); E. Giusarma *et al.*, Phys. Rev. D **83**, 115023 (2011); A.X. Gonzalez-Morales *et al.*, arXiv:1106.5052 [astro-ph.CO]; J. Hamann, arXiv:1110.4271 [astro-ph.CO].
- [8] G. Mangano and P.D. Serpico, Phys. Lett. B **701**, 296 (2011); J. Hamann *et al.*, JCAP **1109**, 034 (2011).
- [9] S. Razzaque and A.Yu. Smirnov JHEP **1107**, 084 (2011); R. Gandhi and P. Ghoshal, arXiv:1108.4360 [hep-ph].
- [10] A.S. Riis and S. Hannestad, JCAP **1102**, 011 (2011); J.A. Formaggio and J. Barrett, arXiv:1105.1326 [nucl-ex].
- [11] See, e.g., James Barry *et al.*, JHEP **1107**, 091 (2011); C. Giunti and M. Laveder, Phys. Rev. D **82**, 053005 (2010); C. Giunti, Phys. Rev. D **61**, 036002 (2000); S.M. Bilenky *et al.*, Phys. Lett. B **465**, 193 (1999).
- [12] W. Rodejohann, Int. J. Mod. Phys. E **20**, 1833 (2011).
- [13] S.M. Bilenky *et al.*, Phys. Rept. **379**, 69 (2003).
- [14] See, e.g., H.V. Klapdor-Kleingrothaus *et al.*, Eur. Phys. J. A **12**, 147 (2001); C.E. Aalseth *et al.* [IGEX Collaboration], Phys. Rev. D **65**, 092007 (2002); C. Arnaboldi *et al.* [CUORICINO Collaboration], Phys. Rev. C **78**, 035502 (2008).
- [15] See, e.g., A. Faessler *et al.*, Phys. Rev. D **83**, 113015 (2011); Phys. Rev. D **79**, 053001 (2009); J. Phys. G **35**, 075104 (2008).
- [16] Z.Z. Xing, Phys. Rev. D **68**, 053002 (2003).
- [17] W. Rodejohann, Nucl.Phys. B **597**, 110 (2001); A. Merle and W. Rodejohann, Phys. Rev. D **73**, 073012 (2006); S. Dev and S.L. Kumar, Mod. Phys. Lett. A **22**, 1401 (2007); J. Jenkins, Phys. Rev. D **79**, 113003 (2009); Y. BenTov and A. Zee, Phys.Rev. D **84**, 073012 (2011).
- [18] G.L. Fogli *et al.*, Phys. Rev. D **84**, 053007 (2011).

- [19] T. Schwetz *et al.*, New J. Phys. **13**, 109401 (2011).
- [20] E. Komatsu *et al.* (WMAP Collaboration), Astrophys. J. Supp. **192**, 18 (2011).
- [21] Y.Y.Y. Wong, Ann. Rev. Nucl. Part. Sci. **61**, 69 (2011); M.C. Gonzalez-Garcia *et al.*, JHEP **1008**, 117 (2010).
- [22] F. Simkovic *et al.* Phys. Rev. D **82**, 113015 (2010); G.L. Fogli *et al.*, Phys. Rev. D **80**, 015024 (2009); F. Deppisch and H. Pas, Phys. Rev. Lett. **98**, 232501 (2007).
- [23] Z.Z. Xing, Phys. Lett. B **679**, 255 (2009); arXiv:1110.0083 [hep-ph].
- [24] See, e.g., P. Benes *et al.*, Phys. Rev. D **71**, 077901 (2005); A.de Gouvea *et al.*, Phys. Rev. D **75**, 013003 (2007); W. Rodejohann, Phys. Lett. B **684**, 40 (2010); M. Blennow *et al.*, JHEP **1007**, 096 (2010); M. Mitra *et al.*, arXiv:1108.0004 [hep-ph].
- [25] C.S. Aulakh and R.N. Mohapatra, Phys. Lett. B **119**, 136 (1982); R.N. Mohapatra, Phys. Rev. D **34** 909 (1986); J.D. Vergados, Phys. Lett. B **184**, 55 (1987).
- [26] H. Ejiri *et al.*, Phys. Rev. Lett. **85**, 2917 (2000); K. Zuber, Phys. Lett. B **519**, 1 (2001); C. Arnaboldi *et al.* [CUORE Collaboration], Astropart. Phys. **20**, 91 (2003); R. Arnold *et al.* [SuperNEMO Collaboration], Eur. Phys. J. C **70**, 927 (2010).
- [27] A. Terashima *et al.* [KamLAND Collaboration], J. Phys. Conf. Ser. **120** 052029 (2008); R. Gaitskell *et al.* [Majorana Collaboration], arXiv:nucl-ex/0311013; M.C. Chen [SNO+ Collaboration], arXiv:0810.3694 [hep-ex].

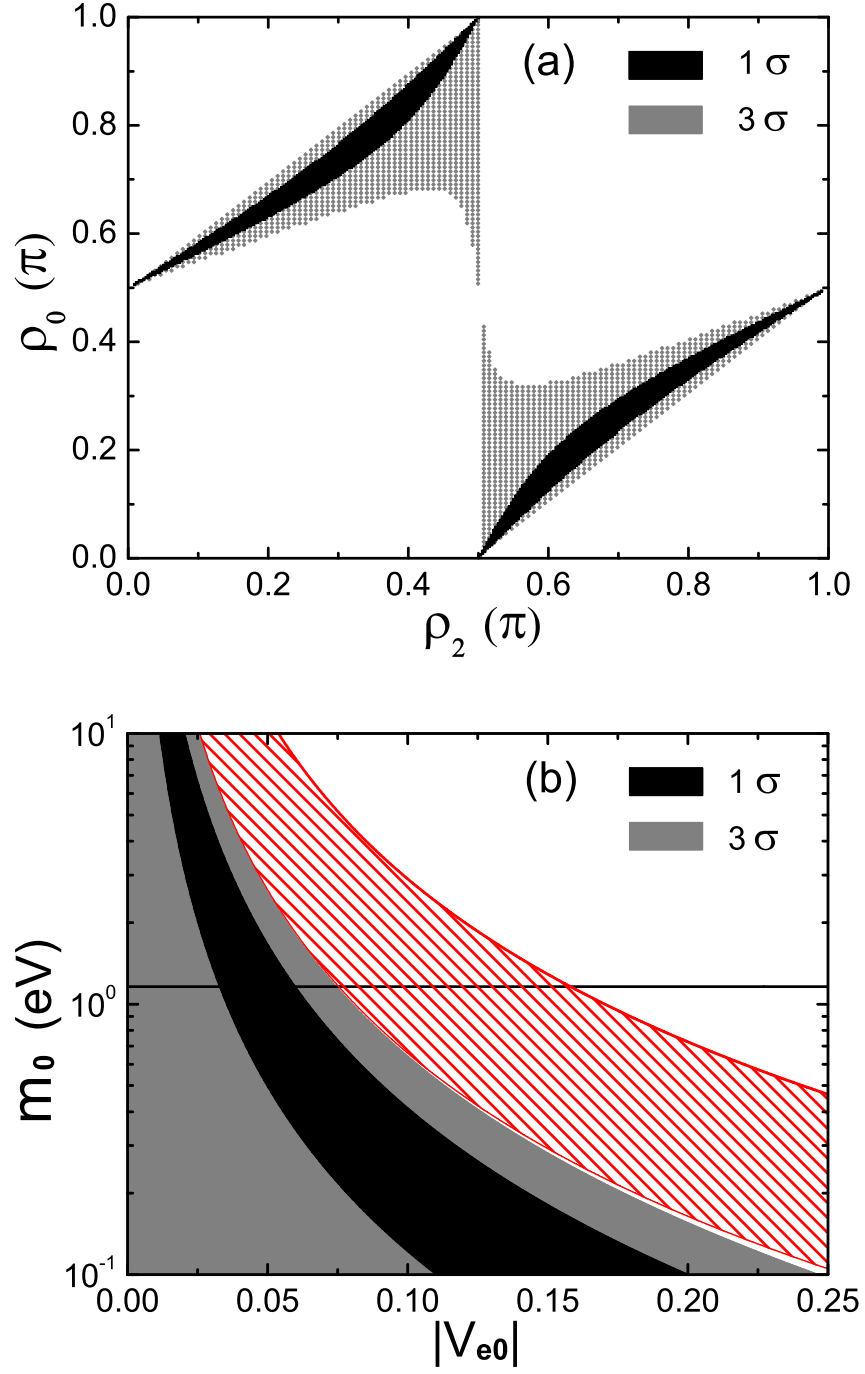


Figure 1: The regions of (ρ_0, ρ_2) (upper panel) and $(m_0, |V_{e0}|)$ (lower panel) allowed by $\langle m \rangle_{ee} = 0$ and current neutrino oscillation data with $\Delta m_{31}^2 > 0$ and $m_1 = 0$. The black and grey scattered regions (upper panel) and shaded regions (lower panel) stand for 1σ and 3σ ranges of the active neutrino data respectively. The region with (red) sparse lines (lower panel) is constrained from the sterile neutrino data. The (black) horizontal line stands for the 2σ upper bound on the sum of the neutrino masses from cosmological probes.

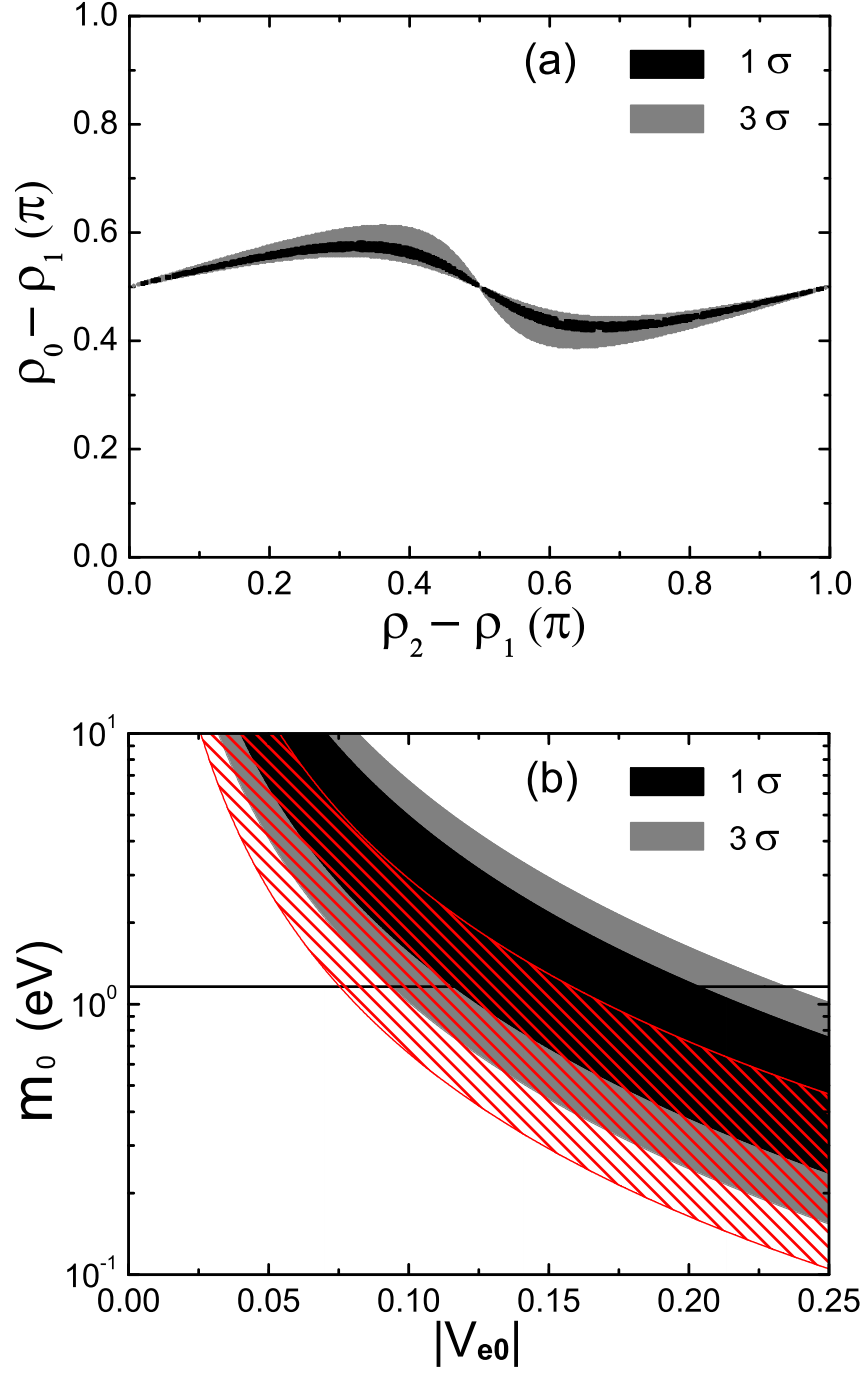


Figure 2: The regions of $(\rho_0 - \rho_1, \rho_2 - \rho_1)$ (upper panel) and $(m_0, |V_{e0}|)$ (lower panel) allowed by $\langle m \rangle_{ee} = 0$ and current neutrino oscillation data with $\Delta m_{31}^2 < 0$ and $m_3 = 0$. The black and grey scattered regions (upper panel) and shaded regions (lower panel) stand for 1σ and 3σ ranges of the active neutrino data respectively. The region with (red) sparse lines (lower panel) is constrained from the sterile neutrino data. The (black) horizontal line stands for the 2σ upper bound on the sum of the neutrino masses from cosmological probes.

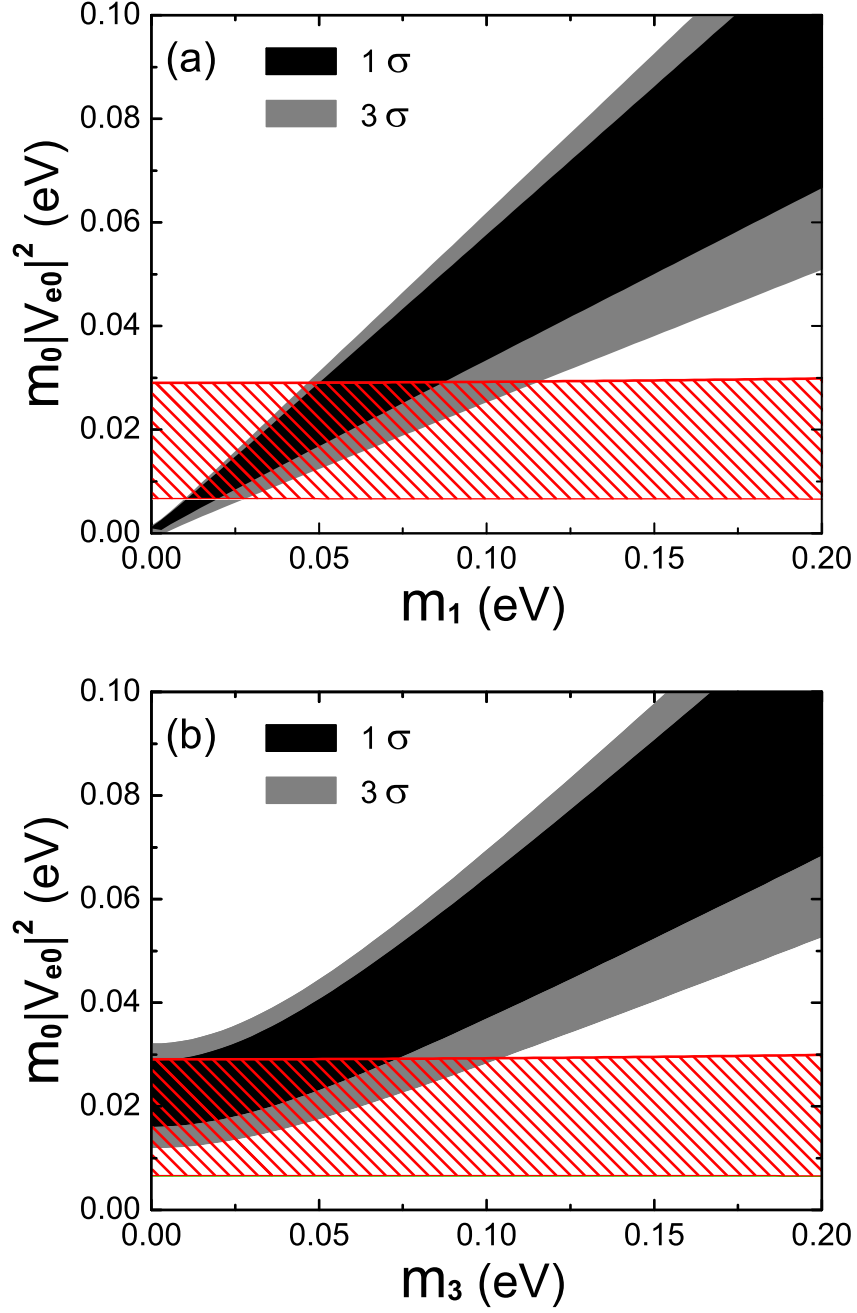


Figure 3: The regions of $m_0|V_{e0}|^2$ versus the smallest neutrino mass (m_1 or m_3) with $\Delta m_{31}^2 > 0$ (upper panel) or $\Delta m_{31}^2 < 0$ (lower panel). The black and grey shaded regions stand for 1σ and 3σ ranges of the active neutrino data respectively. The region with (red) sparse lines is constrained from the sterile neutrino data.

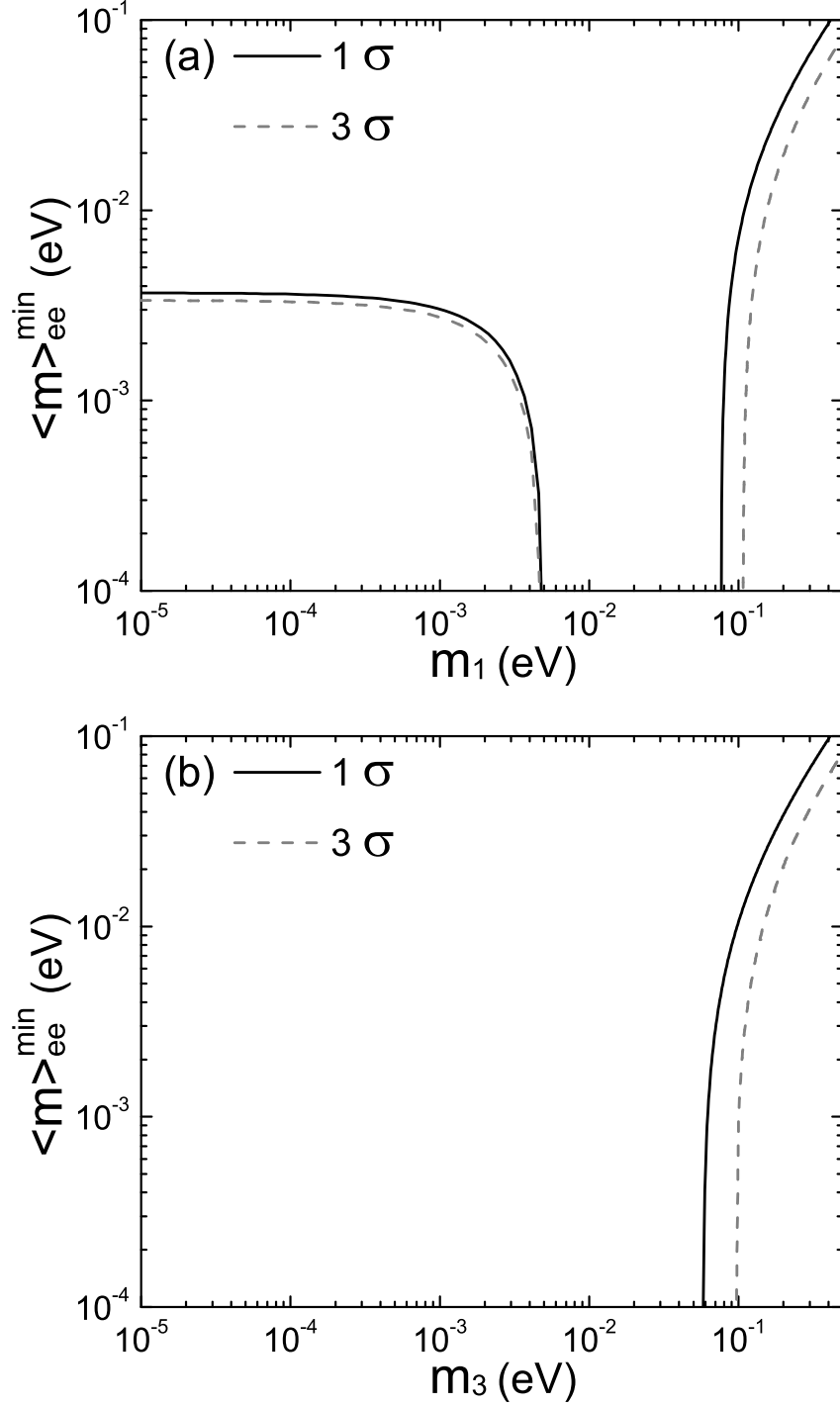


Figure 4: The minimal values of the effective Majorana mass ($\langle m \rangle_{ee}^{\min}$) versus the the smallest neutrino mass (m_1 or m_3) in the $(3 + 2)$ scheme with $\Delta m_{31}^2 > 0$ (upper panel) or $\Delta m_{31}^2 < 0$ (lower panel). The black solid and grey dashed line stand for 1σ and 3σ ranges of the active neutrino data respectively.